

*Climate of the Past Discussions* is the access reviewed discussion forum of *Climate of the Past*

# Low-frequency oscillations of the Atlantic Ocean meridional overturning circulation in a coupled climate model

M. Schulz<sup>1,2</sup>, M. Prange<sup>1,2</sup>, and A. Klockner<sup>1,\*</sup>

<sup>1</sup>Department of Geosciences, University of Bremen, Germany

<sup>2</sup>DFG Research Center “Ocean Margins”, University of Bremen, Germany

\*now at: CSIRO Marine and Atmospheric Research, Hobart, Australia

Received: 15 August 2006 – Accepted: 13 September 2006 – Published: 19 September 2006

Correspondence to: M. Schulz (mschulz@palmod.uni-bremen.de)

CPD

2, 801–830, 2006

AMOC Oscillations

M. Schulz et al.

Title Page

Abstract

Introduction

Conclusions

References

Tables

Figures

⏪

⏩

◀

▶

Back

Close

Full Screen / Esc

Printer-friendly Version

Interactive Discussion

EGU

## Abstract

Using a 3-dimensional climate model of intermediate complexity we show that the overturning circulation of the Atlantic Ocean can vary at multicentennial-to-millennial timescales for present-day boundary conditions. A weak and continuous freshwater input into the Labrador Sea pushes the overturning circulation of the Atlantic Ocean into a bi-stable regime, characterized by phases of active and inactive deep-water formation in the Labrador Sea. In contrast, deep-water formation in the Nordic Seas is active during all phases of the oscillations. The actual timing of the transitions between the two circulation states occurs randomly. The oscillations constitute a 3-dimensional phenomenon and have to be distinguished from low-frequency oscillations seen previously in 2-dimensional models of the ocean. A conceptual model provides further insight into the essential dynamics underlying the oscillations of the large-scale ocean circulation. The model experiments indicate that the coupled climate system can exhibit unforced climate variability at multicentennial-to-millennial timescales that may be of relevance for Holocene and future climate variations.

## 1 Introduction

A number of studies revealed climate variations during the Holocene at timescales ranging from centuries to a few millennia (e.g. Bianchi and McCave, 1999; Bond et al., 1997; Chapman and Shackleton, 2000; Hall et al., 2004; O'Brien et al., 1995; Risebrobakken et al., 2003; Sarnthein et al., 2003; Schulz and Paul, 2002). As the amplitude of these variations is small compared to the pronounced glacial climate variations at similar timescales, an unequivocal detection of such climate fluctuations in climate-proxy records is hampered by comparatively low signal-to-noise ratios and the general shortness of such records. Nevertheless, there seems to be a growing consensus for a recurrence time of climate events in the Holocene ranging from 400–3000 years with a potential clustering around 400–500 years and 900–1100 years (Schulz

CPD

2, 801–830, 2006

## AMOC Oscillations

M. Schulz et al.

Title Page

Abstract

Introduction

Conclusions

References

Tables

Figures

⏪

⏩

◀

▶

Back

Close

Full Screen / Esc

Printer-friendly Version

Interactive Discussion

EGU

et al., 2004, and references therein). Here, the notion of recurrence time only reflects the fact that a record contains a distinct temporal pattern which is repeated after some time. Neither the exact repetition of such a pattern nor an exact timing of its recurrence is implied. Indeed, reported recurrence times vary by as much as approximately  $\pm 50\%$  during the Holocene (Bond et al., 1997; Sarnthein et al., 2003).

The cause of these Holocene climate variations remains elusive. Hypotheses regarding their origin range from internal oscillations of the climate system (e.g. Schulz and Paul, 2002) to external solar-forcing mechanisms (e.g. Bond et al., 2001). Based on analogies to larger-amplitude climate variations and proxy evidence many authors concluded that the Holocene climate fluctuations at centennial-to-millennial timescales, specifically those reconstructed for the North Atlantic region, are linked to changes in the rate of North-Atlantic deep-water production and associated changes in the Atlantic Ocean meridional overturning (AMOC) (e.g. Bond et al., 2001; Oppo et al., 2003). As yet, neither the role of the AMOC in these climate variations has been elucidated – is it cause or effect? – nor the physical mechanism underlying low-frequency AMOC variations.

Understanding the low-frequency oscillations (we use the term oscillation without implying strict periodicity) of Holocene climate change is not only of importance from a paleoclimatic perspective. It is also essential to understand the course and dynamics of these natural climate variations to predict their potential interference with the possible anthropogenic influence on climate (cf. Knutti and Stocker, 2002). Moreover, low-frequency climate variations may be related to the still enigmatic origin of the relatively stable “1500-year” cycle that paced glacial abrupt climate change (Schulz et al., 2004). Therefore, disentangling these interglacial climate fluctuations may also help to better understand glacial climate fluctuations.

Using a coupled climate model of intermediate complexity we show that the AMOC can vary at multicentennial-to-millennial timescales for present-day boundary conditions. The AMOC oscillations result from perturbations of deep-water formation in the Labrador Sea by a weak and constant local freshwater input that conspires with a

## AMOC Oscillations

M. Schulz et al.

[Title Page](#)[Abstract](#)[Introduction](#)[Conclusions](#)[References](#)[Tables](#)[Figures](#)[⏪](#)[⏩](#)[◀](#)[▶](#)[Back](#)[Close](#)[Full Screen / Esc](#)[Printer-friendly Version](#)[Interactive Discussion](#)

destabilizing low-salinity influx originating from the Nordic Seas. A conceptual model provides further insight into the essential dynamics underlying the AMOC oscillations.

## 2 Setup of the coupled climate-model experiments

To test the potential of the climate system to generate low-frequency climate oscillations, we use the global atmosphere-ocean model ECBilt-CLIO, version 3 (more information about the model including the source code is available from <http://www.knmi.nl/onderzk/CKO/ecbilt.html>). This coupled model of intermediate complexity derives from the atmosphere model ECBilt (Opsteegh et al., 1998) and the ocean and sea-ice model CLIO (Goosse and Fichefet, 1999). The atmospheric component solves the quasi-geostrophic equations with T21 resolution ( $\sim 5.6^\circ$ ) for three layers. The primitive-equation, free-surface ocean component has a horizontal resolution of  $3^\circ$  and 20 levels in the vertical and uses a rotated subgrid in the North Atlantic Ocean to avoid the convergence of meridians near the north pole. It includes parameterizations for mixed-layer dynamics, isopycnal mixing and downsloping currents. The ocean model is coupled to a thermodynamic-dynamic sea-ice model with viscous-plastic rheology. There is no local flux correction in ECBilt-CLIO. However, precipitation over the Atlantic and Arctic basins is reduced by 8.5% and 25%, respectively, and homogeneously redistributed over the North Pacific.

Beside a 5000-yr (year) long control run, simulating the modern (i.e., pre-industrial) climate, we conducted three experiments in which a weak perturbation of approximately 30, 45 and 60 cm/yr, respectively was continuously added to the precipitation field over the southern Labrador Sea. The resulting freshwater forcings amount to 5, 7.5 and 10 mSv (milli-Sverdrup;  $1 \text{ Sv} = 10^6 \text{ m}^3/\text{s}$ ), respectively, which is at least one order of magnitude below the values typically used in freshwater-hosing experiments to yield a complete shut-down of deep-water formation in the North Atlantic (Rahmstorf et al., 2005). The local perturbation was globally compensated to close the mass balance. The applied precipitation anomalies are of the same order of magnitude as the annu-

## AMOC Oscillations

M. Schulz et al.

Title Page

Abstract

Introduction

Conclusions

References

Tables

Figures

◀

▶

◀

▶

Back

Close

Full Screen / Esc

Printer-friendly Version

Interactive Discussion

ally averaged precipitation over the Labrador Sea area in the model which amounts to 43 cm/yr. All other boundary conditions in the sensitivity experiments were kept the same as in the control run. For each sensitivity experiment, the model was integrated for another 8000 yr, starting from the final state of the control run as initial condition. All model results presented below are based on annual mean values.

### 3 Simulation results

In the unperturbed control simulation the strength of the AMOC varies between 20 and 35 Sv with a mean value of 28 Sv and a standard deviation of  $\sim 2$  Sv (Fig. 1, top). Spectral analysis reveals that the variability of the AMOC shows a slight tendency towards characteristic timescales of approximately 12 and 200 years (not shown; see Goosse et al. (2003) for a discussion of the variability in ECBilt-CLIO). Since our main interest is in low-frequency variability, i.e., in timescales of at least a few hundred years, we turn to smoothed AMOC time series in the following. Smoothing was performed with a 101-year wide Hanning filter. For the unperturbed control experiment, the smoothed AMOC strength lies between 25 and 29 Sv (Fig. 1, top).

For the freshwater perturbation of 5 mSv the character of the modeled AMOC changes fundamentally. The forcing gives rise to a bi-modal AMOC distribution with values of approximately 28 and 22 Sv (Fig. 1, top). In the following these states of the AMOC will be referred to as “strong” and “weak” states. It is noteworthy that the AMOC oscillates between two states with positive AMOC values, that is, deep-water formation in the North Atlantic Ocean never ceases during the oscillations. Using an arbitrary threshold value of 25 Sv to separate weak and strong states, we find that the model spends 80% of the time in the strong state. Accordingly, the weak state can be viewed as a perturbation of the strong state, lasting between approximately 100 and 700 years.

If the freshwater forcing is increased to 7.5 mSv the principal bi-modality of the AMOC is maintained (Fig. 1, center). However, with the increased magnitude of the

Title Page

Abstract

Introduction

Conclusions

References

Tables

Figures

⏪

⏩

◀

▶

Back

Close

Full Screen / Esc

Printer-friendly Version

Interactive Discussion

**AMOC Oscillations**

M. Schulz et al.

Title Page

Abstract

Introduction

Conclusions

References

Tables

Figures

◀

▶

◀

▶

Back

Close

Full Screen / Esc

Printer-friendly Version

Interactive Discussion

forcing, the model stays only 33% of the time in the strong state. This suggests a tendency for remaining longer in the weak state as the freshwater forcing in the Labrador Sea increases. In this experiment, a total of six weak-to-strong transitions can be observed. The duration between subsequent transitions (in the order of their appearance) is approximately 540, 1360, 310, 2660, and 2220 years. Finally, by increasing the freshwater perturbation to 10 mSv, the model resides in the strong state for only 14% of the time. Accordingly, the previously identified propensity of the model to stay in the weak state for an increased freshwater perturbation gains further support.

To better understand the origin of the AMOC variations we turn to changes in deep-water formation sites in the North Atlantic Ocean. For the strong state, mixed-layer depth points to two sites where deep mixing and, hence, deep-water formation takes places, namely the Nordic Seas and the Labrador Sea (Fig. 2a). The corresponding meridional overturning streamfunction indicates that approximately 16 Sv of the newly formed deep water in the North Atlantic are exported across 30° S into the Southern Ocean (Fig. 2b). Below this layer, approximately 5 Sv of Antarctic Bottom Water enter the Atlantic basin. Both mixed-layer depth and meridional overturning streamfunction are practically identical between the strong state in the 7.5 mSv experiment (Fig. 2a, b) and the unperturbed control experiment (i.e., before model year 5000), which is therefore not shown. In contrast to the strong state, deep-mixing in the weak state is limited to the Nordic Seas (Fig. 2c), where the mixed-layer depth also increases (cf. Figs. 2a, c). Although the absence of deep-water formation in the Labrador Sea leads to a reduction in the maximum of the meridional overturning streamfunction by 6 Sv (Fig. 2b, d) the export to the Southern Ocean decreases by only 2 Sv to a value of 14 Sv. The changes in deep-water formation in the North Atlantic Ocean have no effect on the inflow of Antarctic Bottom Water which remains at 5 Sv. Mixed-layer depth and meridional overturning streamfunction for the weak and strong states show only negligible differences between the different sensitivity experiments. Hence, we limit the presentation of results to those shown in Fig. 2.

The cessation of deep-water formation in the Labrador Sea in the weak state causes

**AMOC Oscillations**

M. Schulz et al.

Title Page

Abstract

Introduction

Conclusions

References

Tables

Figures

◀

▶

◀

▶

Back

Close

Full Screen / Esc

Printer-friendly Version

Interactive Discussion

5 a drop in surface-air temperature in this region by up to 3°C (Fig. 3). At the same time, air temperature rises by up to 1.5°C north of Iceland associated with an increase in oceanic heat transport by approximately 0.05 PW (not shown) due to the slightly enhanced deep-water formation in the Nordic Seas. It should be noted that the zero line between positive and negative temperature anomalies runs through central Greenland as well as Scandinavia (Fig. 3). While the principal pattern of these temperature anomalies is rather stable during the course of the weak state, the actual extent of the anomalies may vary. For example, the warm anomaly may be restricted to Iceland and the area immediately north of it but may not encompass mainland Scandinavia as is the case depicted in Fig. 3 (not shown).

10 In summary, the coupled ocean-atmosphere model exhibits internal oscillations of the AMOC at multicentennial-to-millennial timescales upon weak and continuous freshwater forcing in the Labrador Sea. The oscillations are characterized by a strong state with deep-water formation in both, the Nordic Seas and Labrador Sea and a weak state in which deep water forms only in the Nordic Seas. The minimum (22 Sv) and maximum (28 Sv) values of the AMOC during the oscillations are virtually independent of the magnitude of the freshwater perturbation.

#### 4 Discussion

20 In order to disentangle the dynamics underlying the modeled AMOC oscillations one has to answer the following two questions: (i) why does deep-water formation in the Labrador Sea switch between on and off states? And (ii) what determines the timescale of the oscillations? In our analysis of the model results we will set out from the first question before tackling the second.

## 4.1 Origin of the oscillations

Today, the deep-water formation areas in the Nordic Seas and Labrador Sea are linked through the subpolar gyre, which advects low-salinity surface water from the Arctic Ocean through the East and West Greenland Currents to the Labrador Sea (e.g. Tomczak and Godfrey, 2002). With regard to the model results, the key elements to note are: Firstly, that the deep-water formation site in the Labrador Sea is located “down-stream” of the deep-water formation site in the Nordic Seas. Secondly, that deep-water forms in the Labrador Sea despite the advection of low-salinity water from the “up-stream” area. In other words, today the Nordic Seas exert a destabilizing effect on deep-mixing in the Labrador Sea and, therefore, deep-water formation in that area.

This oceanographic situation is well captured in the model, which resolves the two deep-water formation sites in the North Atlantic Ocean (a condition not always met by coarse-resolution climate models) and advects low-salinity surface water through Denmark Strait into the Labrador Sea. Immediately north of Denmark Strait, near-surface salinity is approximately 1.5 psu lower than in the central Labrador Sea, where deep mixing occurs. The same situation prevails during the strong state of the AMOC oscillations (Fig. 4).

A contrasting situation arises for the weak state, in which a halocline forms in the Labrador Sea that prevents deep mixing. Hence, freshwater entering the Labrador Sea as runoff or precipitation leads to the build-up of a low-salinity surface layer in the Labrador Sea, thus re-enforcing the halocline. Compared to the strong state, near-surface salinity drops by 2 psu to 33 psu in the central Labrador Sea (Fig. 4). At the same time, an anomalous wind pattern (not shown) pushes saline surface water into the Nordic Seas. Subsequent horizontal mixing within the Nordic Seas raises salinity in the Greenland Sea by approximately 0.8 psu. Accordingly, surface salinity north of Denmark Strait is now almost 1.3 psu higher than in the central Labrador Sea (Fig. 4). Advection of this relatively saline water into the Labrador Sea helps to erode the halocline, hence, to re-establish deep-water formation in the Labrador Sea. It should be

Title Page

Abstract

Introduction

Conclusions

References

Tables

Figures

⏪

⏩

◀

▶

Back

Close

Full Screen / Esc

Printer-friendly Version

Interactive Discussion

noted that density variations of the surface-water masses are dominated by salinity variations since average surface temperature vary only little around their mean values of  $-0.3$  and  $-0.6^{\circ}\text{C}$  in the Labrador Sea and Greenland Sea, respectively.

Although the amount of freshwater forcing that moves the model into the oscillating regime will most likely depend on the magnitude of the overturning in the Atlantic Ocean, we surmise that the existence of the oscillation depends less strongly on the overall strength of the oscillations than on the existence of two localities for deep-water formation. Accordingly, we consider the relatively large value of the AMOC in the control experiment (cf. Sect. 3) only of minor importance with respect to the existence of the oscillations.

In summary, independently of the state of the AMOC (weak vs. strong), the “upstream” deep-water formation area in the Nordic Seas tends to destabilize the “downstream” water-column in the Labrador Sea. Thus the switching between the strong and weak states of the AMOC depends critically on the influence that the upstream density reservoir exerts on the downstream reservoir. The lack of AMOC oscillations in the control experiment indicates that the destabilizing effect of the upstream reservoir for modern boundary conditions is insufficient to turn-off the deep mixing in the Labrador Sea. Only when a small amount of freshwater is added to the Labrador Sea, the model crosses a critical threshold and the oscillations appear. In other words, a small positive freshwater anomaly is sufficient to raise the sensitivity of the Labrador Sea to a level allowing a strong response to the influx of low-density water from the upstream reservoir.

Cross-correlating maximum mixed-layer depth in the Labrador Sea with salinity (averaged over the top 50 m) immediately north of Denmark strait provides another way of looking at the proposed link between the two deep-water formation sites (Fig. 5). Salinity and mixed-layer depth show the expected positive correlation and the lead of salinity over mixed-layer depth of approximately 4 years is consistent with the postulated causal link.

Given this explanation of what controls the switching between active and inactive

---

**AMOC Oscillations**M. Schulz et al.

---

[Title Page](#)[Abstract](#)[Introduction](#)[Conclusions](#)[References](#)[Tables](#)[Figures](#)[⏪](#)[⏩](#)[◀](#)[▶](#)[Back](#)[Close](#)[Full Screen / Esc](#)[Printer-friendly Version](#)[Interactive Discussion](#)

deep-water formation in the Labrador Sea, we can now turn to the second question regarding the timing of these switches.

## 4.2 Timescale of the oscillations

The duration between subsequent transitions varies widely from 310 to 2660 years in the 7.5 mSv experiment (Sect. 3; Fig. 1) and does not indicate a preferred timescale within this range. The average duration is approximately 1420 years and the standard deviation amounts to 1020 years. Hence, the total range of values is almost completely covered by the interval of one standard deviation around the mean, supporting the notion that the durations are more or less uniformly distributed (with only 5 durations at hand, no meaningful statistical test of the distribution can be performed). The lack of a dominant timescale argues against a deterministic process controlling the timing of the AMOC oscillations and is easier to reconcile with a stochastic origin. (We use the term “stochastic” in a somewhat loose sense. In the model any “randomness” is generated by the interactions of deterministic processes which lead to high-frequency noise. The build-in random-generator, that can be used to parameterize “weather” in ECBilt-CLIO, was switched off in all experiments.)

Starting from a state with active deep-water formation in the Labrador Sea, a randomly occurring negative density anomaly of sufficient magnitude will reduce vertical mixing for example only in a single grid cell of the model. Due to the strong non-linear feedback associated with vertical mixing (e.g. Rahmstorf, 1995) a complete cessation of vertical mixing in the entire Labrador Sea can then result. For the control experiment this situation apparently never arises, suggesting that the magnitude of the random perturbations is insufficient to cause a transition within the integration period. One can assess the magnitude of the perturbations that occur in the control experiment from the surface density distribution in the Labrador Sea (Fig. 6). From this data, the probability that density falls below  $27.35 \text{ kg/m}^3$  is practically zero. A different situation arises when the Labrador Sea is perturbed by continuous freshwater input in the 5, 7.5 and 10 mSv experiments. While these perturbations by themselves are insufficient to shut down

Title Page

Abstract

Introduction

Conclusions

References

Tables

Figures

⏪

⏩

◀

▶

Back

Close

Full Screen / Esc

Printer-friendly Version

Interactive Discussion

convection permanently, they make deep-water formation in the Labrador Sea more vulnerable to the randomly occurring negative density anomalies. It is the combined effect of the continuous freshwater forcing together with random density anomalies that has the potential for bringing deep-water formation to a halt. Once convection has ceased, lateral advection of water masses with relatively high densities, originating partly in the Nordic Seas (cf. Fig. 4), will start to erode the halocline that prevents deep-mixing in the Labrador Sea. As for the shutdown of deep-water formation it is, however, the superimposed effect of positive density anomalies occurring at random that ultimately re-initiate convection in the Labrador Sea.

Given the noise-induced transitions between the states with and without convection in the Labrador Sea, the change in the ratio of the duration of strong state to weak state of the AMOC oscillations (cf. Fig. 1) can be explained. Starting from a strong state, a larger value of the continuous freshwater forcing brings the Labrador Sea closer to the point at which a random negative density anomaly can stop the deep mixing. Thus the probability for a shutdown of convection in the Labrador Sea increases with increasing freshwater forcing. The histograms for the density anomalies in the Labrador Sea provide further evidence for this. For larger freshwater forcing, the high-density mode, associated with the strong mode, becomes more negatively skewed, making transitions from the strong to the weak mode more likely (Fig. 6).

Once the system is in the weak mode, the likelihood for a large positive density anomaly determines how long this mode prevails. Since a larger freshwater forcing moves the Labrador Sea towards less dense surface waters, the probability for a weak-to-strong transition decreases with increasing freshwater forcing. This effect of the freshwater forcing can also be inferred from the histograms which show that the peak associated with the weak mode is shifted towards smaller densities for increasing values of the freshwater forcing (Fig. 6). In summary, the larger the freshwater forcing, the more likely is a transition from strong to weak modes and the more unlikely is a mode switch in the opposite direction. For the 7.5 mSv forcing the tails of both peaks in the histogram clearly overlap, making transitions between both states likely to occur in

**AMOC Oscillations**

M. Schulz et al.

[Title Page](#)[Abstract](#)[Introduction](#)[Conclusions](#)[References](#)[Tables](#)[Figures](#)[⏪](#)[⏩](#)[◀](#)[▶](#)[Back](#)[Close](#)[Full Screen / Esc](#)[Printer-friendly Version](#)[Interactive Discussion](#)

each direction. The change in the likelihood for each state with varying freshwater forcing manifests itself in the shift in the ratio between strong and weak modes discussed above (cf. Fig. 1).

#### 4.3 Conceptual model of the oscillations

5 Probably the simplest model that captures the basic mechanisms of the low-frequency oscillations consists of two prognostic variables,  $T$  and  $S$ , representing spatially averaged temperature and salinity of the upper (say, the topmost 200 m) Labrador Sea. Hydrographic conditions in the upper Labrador Sea depend on the wind- and density-driven inflows from the subtropical Atlantic, the influx of subpolar water from the Greenland Sea (via the East Greenland Current through Denmark Strait) and surface fluxes. The deterministic governing equations for Labrador Sea temperature and salinity can therefore be formulated as

$$\frac{dS}{dt} = \frac{1}{V} [(q_1 + \Phi) S_1 + q_2 S_2 - (q_1 + q_2 + \Phi + P + P') S] , \quad (1)$$

$$\frac{dT}{dt} = \frac{1}{V} [(q_1 + \Phi) T_1 + q_2 T_2 - (q_1 + q_2 + \Phi) T] + H , \quad (2)$$

15 where  $V$  denotes the volume of the upper Labrador Sea ( $3 \cdot 10^{14} \text{ m}^3$ ),  $q_1$  is the wind-driven volume flux from the subtropical Atlantic,  $\Phi$  is the density-driven (overturning) volume flux from the subtropical Atlantic,  $q_2$  is the volume flux from the Greenland Sea,  $P$  denotes a basic surface freshwater flux into the Labrador Sea (78 mSv),  $P'$  is a freshwater flux perturbation,  $H$  denotes the surface heat flux, and  $t$  is time.  $S_1$ ,  $T_1$  and  $S_2$ ,  $T_2$  denote salinities and temperatures of the inflowing subtropical and subpolar water masses, respectively. To keep the model as simple as possible, the wind-driven volume fluxes are assumed to be constant ( $q_1 = 2 \text{ Sv}$ ,  $q_2 = 2 \text{ Sv}$ ; after Fig. 10.50 in Dietrich, 1975). Likewise, any temperature and salinity changes in the water masses originating from the subtropical Atlantic and the Greenland Sea are neglected ( $S_1 = 35.3 \text{ psu}$ ,  $T_1 = 8^\circ\text{C}$ ,  $S_2 = 34.6 \text{ psu}$ ,  $T_2 = 1.5^\circ\text{C}$ ). The overturning  $\Phi$  couples the pair of differential

Title Page

Abstract

Introduction

Conclusions

References

Tables

Figures

◀

▶

◀

▶

Back

Close

Full Screen / Esc

Printer-friendly Version

Interactive Discussion

## AMOC Oscillations

M. Schulz et al.

equations through a linear dependence on the density difference between the Labrador Sea and the subtropical Atlantic, i.e.  $\Phi = \kappa [\alpha (T_1 - T) - \beta (S_1 - S)]$ , where  $\alpha$  and  $\beta$  denote the thermal and haline expansion coefficients of seawater ( $\alpha = 0.1 \text{ K}^{-1}$ ,  $\beta = 0.8 \text{ psu}^{-1}$ ). The tuning parameter  $\kappa$  is set to 70 Sv. If  $\Phi$  becomes lower than zero,  $\Phi$  is set to zero (state of no overturning or “off” mode). For the surface heat flux  $H$ , a simple restoring term is used, i.e.,  $H = (\Theta - T) / \tau$ , where  $\Theta = 0^\circ\text{C}$  is a relaxation temperature and  $\tau = 1 \text{ yr}^{-1}$  is the relaxation time scale. This simple approach parameterizes the damping of surface temperature anomalies by atmospheric heat advection and/or longwave radiation. An analogy for salinity does not exist since the atmosphere is insensitive to the presence of salinity anomalies.

In order to analyze the stability behavior of the simple deterministic model, an equilibrium hysteresis with respect to surface freshwater forcing is calculated. It is well known that the competition between thermal and saline forcings of the overturning may result in multiple equilibria (Stommel, 1961). Plotting the overturning  $\Phi$  against the anomalous freshwater forcing  $P'$  reveals a regime of bi-stability for intermediate forcing amplitudes (Fig. 7). With  $P' = 0 \text{ Sv}$ , for instance, one stable equilibrium (“off” mode) has zero overturning and a Labrador Sea salinity of  $S \cong 34.3 \text{ psu}$ , while the other stable equilibrium (“on” mode) yields an overturning of  $\Phi = 10 \text{ Sv}$  and a salinity of  $\sim 35.0 \text{ psu}$ . For very large positive/negative values of  $P'$ , only the “off”/“on” mode of Labrador Sea overturning provides a stable solution. Since the inflow of subpolar water ( $S_2 = 34.6 \text{ psu}$ ) has a higher/lower salinity than the Labrador Sea in the “off”/“on” mode, it has a destabilizing effect on the respective state of overturning. To demonstrate this, we calculate another equilibrium hysteresis with  $q_2$  set to zero (Fig. 7, red curve). As a result of the missing northern inflow, the hysteresis loop widens, i.e., larger positive or negative freshwater perturbations  $P'$  are necessary to induce a transition from one mode to the other.

The simple model possesses no internal variability. In the bi-stable regime of ocean circulation, however, occasional state transitions can be introduced by a stochastic forcing component (cf. Cessi, 1994). We add a term  $\sigma \xi S_0 / V$  to Eq. (1) to introduce a stochastic component in the salinity balance, where  $\xi$  represents Gaussian “quasi

Title Page

Abstract

Introduction

Conclusions

References

Tables

Figures

◀

▶

◀

▶

Back

Close

Full Screen / Esc

Printer-friendly Version

Interactive Discussion

## AMOC Oscillations

M. Schulz et al.

Title Page

Abstract

Introduction

Conclusions

References

Tables

Figures

◀

▶

◀

▶

Back

Close

Full Screen / Esc

Printer-friendly Version

Interactive Discussion

white noise” with zero mean and unit variance (a non-vanishing autocorrelation up to 3 days is introduced by the 3-days time step of the Euler forward scheme used to solve the differential equations),  $\sigma$  measures the standard deviation of the stochastic forcing and  $S_0$  denotes a reference salinity (35 psu). Setting  $\sigma=0.2$  Sv and applying no additional freshwater flux ( $P'=0$  Sv), we obtain numerous transitions from one mode to the other during a 50 000 year integration, resulting in multacentennial-to-millennial variations of the overturning circulation (Fig. 8). The mean residence time in a circulation mode before switching back to the other state (or the Kramers rate) and, hence, the timescale of the oscillations is given by the noise intensity (cf. Cessi, 1994). The stronger the noise, the larger is the probability for a flip into the other equilibrium, and the shorter is the mean residence time in one mode. Note, however, that the underlying bi-stability of the deterministic system may be completely masked if the amplitude of the stochastic forcing is too strong (cf. Monahan, 2002; Stommel and Young, 1993). For  $\sigma=0.2$  Sv, the oscillations produced by the simple stochastic model are very similar to the oscillations observed in ECBilt-CLIO (given that the “off”/ “on” mode of the conceptual model corresponds to the weak/strong mode in ECBilt-CLIO, where Labrador Sea convection is switched off/on). Moreover, the conceptual model captures the response of the 3-dimensional climate model to additional constant freshwater inputs. With positive/negative constant perturbation, the system spends more time in the “off”/“on” mode (Fig. 8, left column; Fig. 9), since larger random perturbations are required to induce a transition to the “on”/“off” mode. In the absence of a subpolar water inflow from the Greenland Sea ( $q_2=0$  Sv) state transitions become unlikely (Fig. 8, right column) due to the different stability behavior of the system associated with the wider hysteresis loop. In other words, the inflow from the Greenland Sea via Denmark Strait favors stochastic switches from one mode to the other.

With Greenland Sea inflow a systematic relationship emerges between the mean residence- time ratio (i.e., the ratio between the mean residence times in the “off” mode and the “on” mode) and the constant freshwater perturbation  $P'$  (Fig. 9). The higher the anomalous freshwater input into the Labrador Sea, the longer is the mean residence

time in the “off” mode. Histograms of Labrador Sea density show, however, that both modes are significantly populated for a certain range of constant freshwater input  $P'$  (Fig. 10). Over this  $P'$ -range, small freshwater inputs shift the frequency from the high- to the low-density mode of the probability density function – exactly as in ECBilt-CLIO (Fig. 6). For large freshwater inputs, the bi-modal structure of the probability density vanishes (not shown). Note that the variance of the “off” mode distribution is larger than that of the “on” mode, as it is in ECBilt-CLIO. This is due to a regulation of Labrador Sea density by the overturning circulation on short timescales which is only active in the “on” mode: if Labrador Sea density increases, the overturning and hence the inflow of warm, low-density subtropical water increases, counteracting the initial density increase in the Labrador Sea. The conceptual model is able to capture this mechanism due to the inclusion of a variable Labrador Sea temperature (Eq. 2).

In summary, the simple non-linear stochastic model reproduces the low-frequency oscillations observed in ECBilt-CLIO. It captures not only the occasional transitions from one equilibrium to the other, but also the variance of the fluctuations around each state. In doing so, it is capable to elucidate the physics behind the oscillations found in ECBilt-CLIO. These oscillations can be attributed to an underlying bi-stability in Labrador Sea convection and state transitions induced by noise. A slightly more complex approach for a conceptual model could have accounted for variations in Greenland Sea salinity variations. As shown in Fig. 4, Greenland Sea salinity slightly varies between the weak and strong mode in ECBilt-CLIO (substantial variations in subtropical salinities have not been found). An increase/decrease in Greenland Sea salinity in the “off”/“on” mode would have a destabilizing effect on the respective state of circulation. In other words, the equilibrium hysteresis would become narrower as compared to the case with fixed Greenland Sea salinity. This would favor state transitions under stochastic forcing, resulting in a higher frequency of the oscillations. A reduction in the noise intensity  $\sigma$  could compensate for this effect, leading to the same oscillations as those presented in Fig. 8. The conclusions drawn from our minimal model would be largely unaffected.

## AMOC Oscillations

M. Schulz et al.

Title Page

Abstract

Introduction

Conclusions

References

Tables

Figures

◀

▶

◀

▶

Back

Close

Full Screen / Esc

Printer-friendly Version

Interactive Discussion

---

**AMOC Oscillations**M. Schulz et al.

---

[Title Page](#)[Abstract](#)[Introduction](#)[Conclusions](#)[References](#)[Tables](#)[Figures](#)[⏪](#)[⏩](#)[◀](#)[▶](#)[Back](#)[Close](#)[Full Screen / Esc](#)[Printer-friendly Version](#)[Interactive Discussion](#)

The timescale of the oscillations in our experiments is similar to those resulting from so-called “deep-decoupling oscillations” (Winton, 1997). Nevertheless, the two types of oscillations have to be clearly distinguished. The oscillations described here are intrinsically linked to the 3-dimensional flow field of the Atlantic Ocean and constitute a type of oscillations that has to our knowledge not been observed previously in models.

With respect to reconstructed climate variations during the Holocene, our results suggest a potential mechanism to explain the observed low-frequency variability by an internal mechanism. However, such an interpretation immediately leads to the question, which mechanism moves the system into the bi-stable regime (i.e., provides the continuous freshwater forcing to the Labrador Sea). The simplest answer may be that the Holocene climate has been in this mode for most of the time and that the random nature and small amplitude of the oscillations simply hampered their unequivocal detection. It may equally well be that the internal oscillations get phase-locked to external (e.g. solar) forcing at multicentennial timescales (Bond et al., 2001), thus providing an amplifier for the inferred solar forcing of Holocene climate change. The potential of this mechanism with respect to Holocene climate variability will be the subject of a forthcoming study.

## 5 Summary and conclusions

Our model experiments suggest that interactions between the Nordic Seas and the Labrador Sea can result in oscillations of the overturning circulation of the Atlantic Ocean at multicentennial-to-millennial timescales. A weak and continuous freshwater input into the Labrador Sea can push the large-scale ocean circulation into a bi-stable regime, which is characterized by phases of active and inactive deep-water formation in the Labrador Sea. In contrast, deep-water formation in the Nordic Seas is active during all phases of the oscillations. The near-surface flow through Denmark Strait couples the two deep-water formation regions through the advection of density anomalies which always tend to destabilize the deep-water formation mode of the Labrador

Sea. The actual timing of the transitions between the circulation states occurs randomly. The oscillations constitute a 3-dimensional phenomenon and have to be clearly distinguished from low-frequency oscillations seen previously in 2-dimensional models of the ocean.

Whether or not the oscillations described in this study did occur in the past, can be tested by contrasting deep-water formation proxies from the Labrador Sea and the Nordic Seas. Moreover, based on the predicted surface-air temperature variations, it appears that central Greenland is rather insensitive to monitor the changes. Indeed, our results suggest that temperature records from the Nordic Seas could provide much stronger evidence for the oscillations.

The proposed oscillation mechanism may also be of relevance with respect to future climate change. Based on model experiments it has been suggested that runoff from Greenland into the Labrador Sea may increase in the future (Huybrechts et al., 2004). Although associated with large uncertainties, the estimated freshwater forcing is on the order of a few milli-Sverdrups. If the AMOC is currently indeed in the bi-stable regime, our model experiments imply that, in the future, the AMOC would reside more frequently in the weak mode. In contrast, if the system is currently not in the bi-stable regime, the additional freshwater forcing may push the AMOC into the oscillating regime. In any case, future climate could be associated with low-frequency oscillations of the AMOC rather than the frequently envisioned weakening or shutdown (IPCC, 2001) (Fig. 11). Experiments with other 3-dimensional climate models, specifically more comprehensive models, should therefore be carried out, to test the robustness of the mechanism that gives rise to the low-frequency AMOC oscillations in our climate model of intermediate complexity.

*Acknowledgements.* We thank P. Herrmann for developing most useful netCDF routines for ECBilt-CLIO and H. Goosse for his continued improvement of the model. This work was supported by the Deutsche Forschungsgemeinschaft through DFG Research Center "Ocean Margins". This is RCOM publication #####.

## AMOC Oscillations

M. Schulz et al.

Title Page

Abstract

Introduction

Conclusions

References

Tables

Figures

◀

▶

◀

▶

Back

Close

Full Screen / Esc

Printer-friendly Version

Interactive Discussion

## References

- Bianchi, G. G. and McCave, I. N.: Holocene periodicity in North Atlantic climate and deep-ocean flow south of Iceland, *Nature*, 397, 515–517, 1999.
- Bond, G., Kromer, B., Beer, J., Muscheler, R., Evans, M. N., Showers, W., Hoffmann, S., Lotti-  
5 Bond, R., Hajdas, I., and Bonani, G.: Persistent solar influence on North Atlantic climate during the Holocene, *Science*, 294, 2130–2136, 2001.
- Bond, G., Showers, W., Cheseby, M., Lotti, R., Almasi, P., deMenocal, P., Priore, P., Cullen, H., Hajdas, I., and Bonani, G.: A pervasive millennial-scale cycle in North Atlantic Holocene and glacial climates, *Science*, 278, 1257–1266, 1997.
- 10 Cessi, P.: A simple box model of stochastically forced thermohaline flow, *J. Phys. Oceanogr.*, 24, 1911–1920, 1994.
- Chapman, M. R. and Shackleton, N. J.: Evidence of 550-year and 1000-year cyclicities in North Atlantic circulation patterns during the Holocene, *The Holocene*, 10, 287–291, 2000.
- Dietrich, G., Kalle, K., Krauss, W., and Siedler, G.: *Allgemeine Meereskunde*, Gebr. Borntraeger, Berlin, 593, 1980.
- 15 Goosse, H. and Fichefet, T.: Importance of ice-ocean interactions for the global ocean circulation: A model study, *J. Geophys. Res.*, C104, 23 337–23 355, 1999.
- Goosse, H., Selten, F. M., Haarsma, R. J., and Opsteegh, J. D.: Large sea-ice volume anomalies simulated in a coupled climate model, *Climate Dynamics*, 20, 523–536, 2003.
- 20 Hall, I. R., Bianchi, G. G., and Evans, J. R.: Centennial to millennial scale Holocene climate-deep water linkage in the North Atlantic, *Quat. Sci. Rev.*, 23, 1529–1536, 2004.
- Huybrechts, P., Gregory, J., Janssens, I., and Wild, M.: Modelling Antarctic and Greenland volume changes during the 20th and 21st centuries forced by GCM time slice integrations, *Global and Planetary Change*, 42, 83–105, 2004.
- 25 IPCC: *Climate Change 2001: Synthesis Report*, A Contribution of Working Groups I, II, and III to the Third Assessment Report of the Intergovernmental Panel on Climate Change, pp. 398, Cambridge University Press, Cambridge, 2001.
- Knutti, R. and Stocker, T. F.: Limited predictability of future thermohaline circulation close to an instability threshold, *Journal of Climate*, 15, 179–186, 2002.
- 30 Monahan, A. H.: Stabilisation of climate regimes by noise in a simple model of the thermohaline circulation, *J. Phys. Oceanogr.*, 32, 2072–2085, 2002.
- O'Brien, S. R., Mayewski, P. A., Meeker, L. D., Meese, D. A., Twickler, M. S., and Whitlow, S. I.:

CPD

2, 801–830, 2006

## AMOC Oscillations

M. Schulz et al.

Title Page

Abstract

Introduction

Conclusions

References

Tables

Figures

◀

▶

◀

▶

Back

Close

Full Screen / Esc

Printer-friendly Version

Interactive Discussion

EGU

## AMOC Oscillations

M. Schulz et al.

[Title Page](#)[Abstract](#)[Introduction](#)[Conclusions](#)[References](#)[Tables](#)[Figures](#)[⏪](#)[⏩](#)[◀](#)[▶](#)[Back](#)[Close](#)[Full Screen / Esc](#)[Printer-friendly Version](#)[Interactive Discussion](#)

Complexity of Holocene climate as reconstructed from a Greenland ice core, *Science*, 270, 1962–1964, 1995.

Oppo, D. W., McManus, J. F., and Cullen, J. L.: Deepwater variability in the Holocene epoch, *Nature*, 422, 277–278, 2003.

5 Opsteegh, J. D., Haarsma, R. J., Selten, F. M., and Kattenberg, A.: ECBILT: a dynamic alternative to mixed boundary conditions in ocean models, *Tellus 50A*, 348–367, 1998.

Rahmstorf, S.: Bifurcations of the Atlantic thermohaline circulation in response to changes in the hydrological cycle, *Nature*, 378, 145–149, 1995.

10 Rahmstorf, S., Crucifix, M., Ganopolski, A., Goosse, H., Kamenkovich, I., Knutti, R., Lohmann, G., Marsh, R., Mysak, L. A., Wang, Z., and Weaver, A. J.: Thermohaline circulation hysteresis: A model intercomparison, *Geophys. Res. Lett.*, 32, L23605, 10.1029/2005GL023655, 2005.

Risebrobakken, B., Jansen, E., Andersson, C., Mjelde, E., and Hevrøy, K.: A high-resolution study of Holocene paleoclimatic and paleoceanographic changes in the Nordic Seas, *Paleoceanography*, 18, 1017, doi:10.1029/2002PA000764, 2003.

15 Sarnthein, M., van Kreveld, S., Erlenkeuser, H., Grootes, P., Kucera, M., Pflaumann, U., and Schulz, M.: Centennial-to-millennial-scale periodicities of Holocene climate and sediment injections off the western Barents shelf, 75° N, *Boreas*, 32, 447–461, 2003.

Schulz, M. and Paul, A.: Holocene climate variability on centennial-to-millennial time scales: 1. Climate records from the North-Atlantic realm, in: *Climate development and history of the North Atlantic Realm*, edited by: Wefer, G., Berger, W. H., Behre, K. E., and Jansen, E., pp. 41–54, Springer Verlag, Berlin, 2002.

20 Schulz, M., Paul, A., and Timmermann, A.: Glacial-Interglacial Contrast in Climate Variability at Centennial-to-Millennial Timescales: Observations and Conceptual Model, *Quat. Sci. Rev.*, 23, 2219–2230, 2004.

25 Stommel, H.: Thermohaline convection with two stable regimes of flow, *Tellus*, 13, 224–228, 1961.

Stommel, H. and Young, W.: The average T-S relation of a stochastically-forced box model, *J. Phys. Oceanogr.*, 23, 151–158, 1993.

30 Tomczak, M. and Godfrey, J. S.: Regional oceanography: an introduction, pp. 391, 2002.

Winton, M.: The effect of cold climate upon North Atlantic Deep Water formation in a simple ocean-atmosphere model, *J. Clim.*, 10, 37–51, 1997.

## AMOC Oscillations

M. Schulz et al.

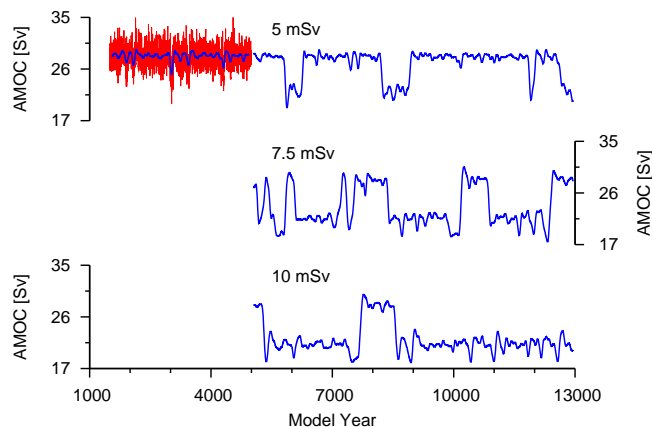


**Fig. 1.** Time series of the maximum of the North Atlantic Ocean meridional overturning (AMOC), calculated north of  $30^{\circ}$  N and below 500 m water depth. Positive values indicate poleward flow in the upper branch of the overturning cell. (Top) Unsmoothed annual values (red) from the unperturbed control experiment (prior to model year 5000). The corresponding output from a 101-year wide Hanning filter is overlain (blue). After model year 5000 a 5 mSv freshwater perturbation is applied in the Labrador Sea. The resulting AMOC time series (smoothed) oscillates between approximately 22 and 28 Sv. (Center) AMOC for a 7.5 mSv freshwater perturbation starting in model year 5000 (smoothed time series). (Bottom) As before but for a 10 mSv forcing.

[Title Page](#)[Abstract](#)[Introduction](#)[Conclusions](#)[References](#)[Tables](#)[Figures](#)[◀](#)[▶](#)[◀](#)[▶](#)[Back](#)[Close](#)[Full Screen / Esc](#)[Printer-friendly Version](#)[Interactive Discussion](#)

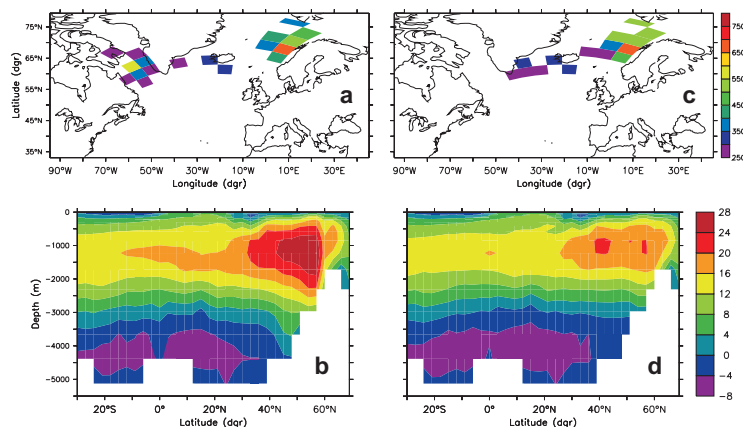


**Fig. 2.** Mixed-layer depth and meridional overturning streamfunction in the Atlantic Ocean. (a) Mixed-layer depth [m] for the strong state, with deep mixing in the Labrador Sea and Nordic Seas. (b) Meridional overturning streamfunction [Sv] for the strong state. Positive values indicate clockwise rotation. (c, d) As a, b but for the weak state without deep-water formation in the Labrador Sea. All plots are based on annual mean values from the 7.5 mSv experiment, averaged over model years 8000–8050 (strong state) and 8900–8950 (weak state).

[Title Page](#)[Abstract](#)[Introduction](#)[Conclusions](#)[References](#)[Tables](#)[Figures](#)[◀](#)[▶](#)[◀](#)[▶](#)[Back](#)[Close](#)[Full Screen / Esc](#)[Printer-friendly Version](#)[Interactive Discussion](#)

## AMOC Oscillations

M. Schulz et al.

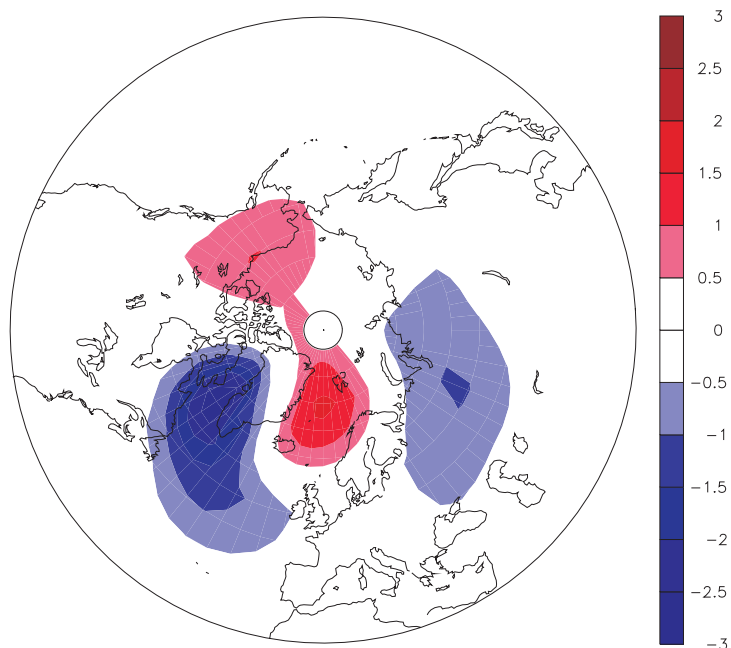


**Fig. 3.** Near-surface (2 m) air-temperature difference [ $^{\circ}\text{C}$ ] between weak state and strong state in the northern hemisphere. Anomalies are based on annual mean values from the 7.5 mSv experiment, averaged over model years 8000–8050 (strong state) and 8900–8950 (weak state).

[Title Page](#)[Abstract](#)[Introduction](#)[Conclusions](#)[References](#)[Tables](#)[Figures](#)[◀](#)[▶](#)[◀](#)[▶](#)[Back](#)[Close](#)[Full Screen / Esc](#)[Printer-friendly Version](#)[Interactive Discussion](#)

## AMOC Oscillations

M. Schulz et al.

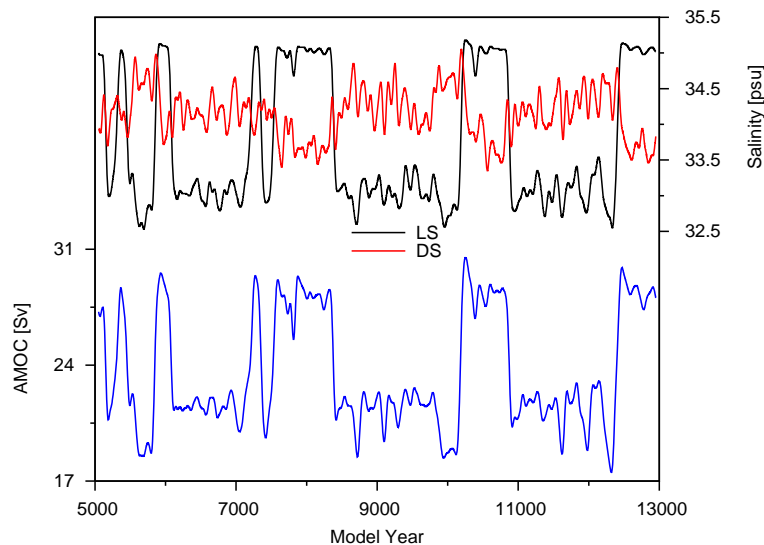


**Fig. 4.** Surface-salinity variations in the North Atlantic Ocean and meridional overturning in the 7.5 mSv experiment. (Top) Salinity immediately north of Denmark Strait (DS, red) and in the central Labrador Sea (LS, black). Salinities are averaged from the surface to 50 m depth. (Bottom) Meridional overturning (as in Fig. 1, center). All time series are smoothed by a 101-year wide Hanning filter.

[Title Page](#)[Abstract](#)[Introduction](#)[Conclusions](#)[References](#)[Tables](#)[Figures](#)[◀](#)[▶](#)[◀](#)[▶](#)[Back](#)[Close](#)[Full Screen / Esc](#)[Printer-friendly Version](#)[Interactive Discussion](#)

## AMOC Oscillations

M. Schulz et al.

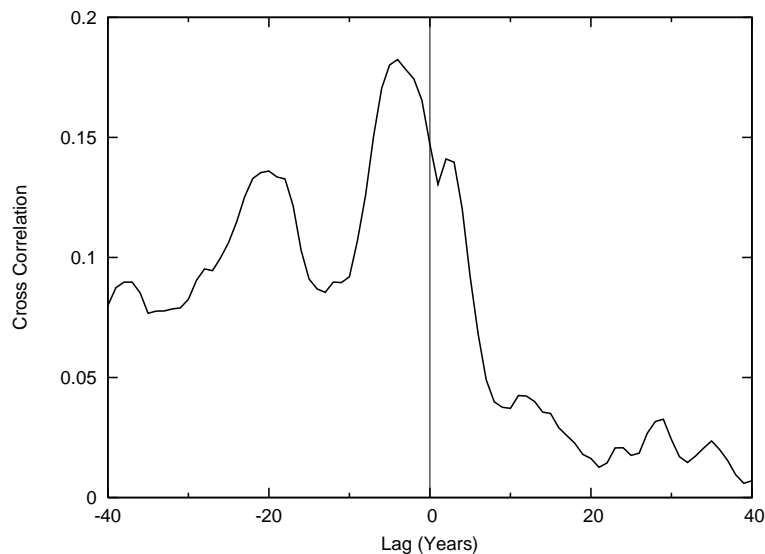


**Fig. 5.** Cross correlation between maximum mixed-layer depth in the Labrador Sea and surface salinity (averaged over top 50 m) immediately north of Denmark Strait. Maximum of the correlation function at a lag of  $-4$  years indicates that salinity anomalies precede mixed-layer anomalies by this amount of time. Analysis based on annual mean values.

[Title Page](#)[Abstract](#)[Introduction](#)[Conclusions](#)[References](#)[Tables](#)[Figures](#)[◀](#)[▶](#)[◀](#)[▶](#)[Back](#)[Close](#)[Full Screen / Esc](#)[Printer-friendly Version](#)[Interactive Discussion](#)

## AMOC Oscillations

M. Schulz et al.

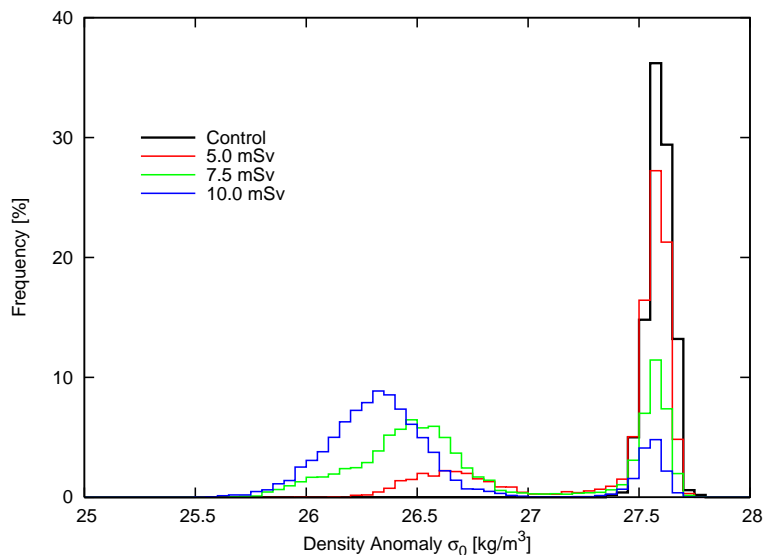


**Fig. 6.** Histogram of surface density anomalies in the central Labrador Sea for all experiments. Anomalies (i.e., water density minus  $1000 \text{ kg/m}^3$ ) are averaged from the surface to 50 m depth. The high-density mode at  $27.6 \text{ kg/m}^3$  corresponds to active deep-water formation in the Labrador Sea (“strong” mode), whereas the low-density modes between  $26.3$  and  $26.7 \text{ kg/m}^3$  result when no deep mixing occurs (“weak” mode). Note that the control experiment (black) is characterized by a high-density mode only.

[Title Page](#)[Abstract](#)[Introduction](#)[Conclusions](#)[References](#)[Tables](#)[Figures](#)[◀](#)[▶](#)[◀](#)[▶](#)[Back](#)[Close](#)[Full Screen / Esc](#)[Printer-friendly Version](#)[Interactive Discussion](#)

## AMOC Oscillations

M. Schulz et al.

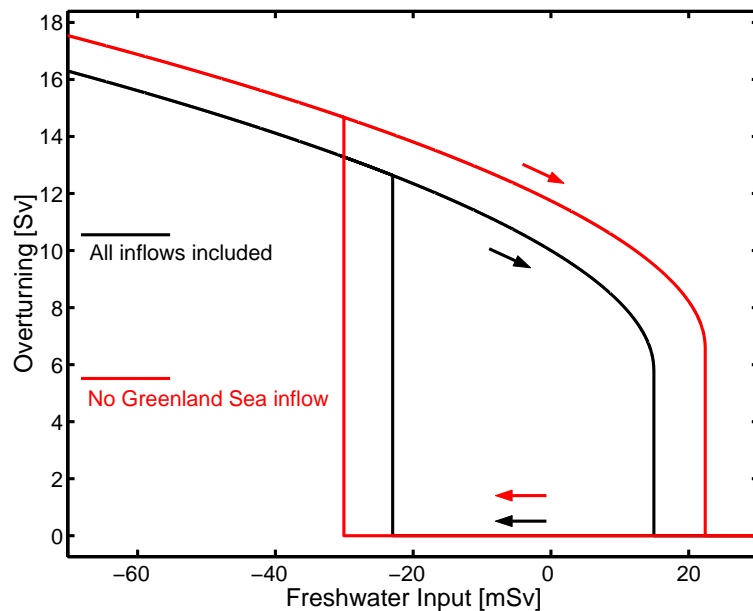


**Fig. 7.** Equilibrium hysteresis loops (Labrador Sea overturning  $\Phi$  vs. freshwater input  $P'$ ) for the deterministic conceptual model with (black) and without (red) inflow from the Greenland Sea to the Labrador Sea. The hysteresis loops have been obtained by slowly varying the freshwater input into the Labrador Sea in the direction indicated by the arrows.

[Title Page](#)[Abstract](#)[Introduction](#)[Conclusions](#)[References](#)[Tables](#)[Figures](#)[◀](#)[▶](#)[◀](#)[▶](#)[Back](#)[Close](#)[Full Screen / Esc](#)[Printer-friendly Version](#)[Interactive Discussion](#)

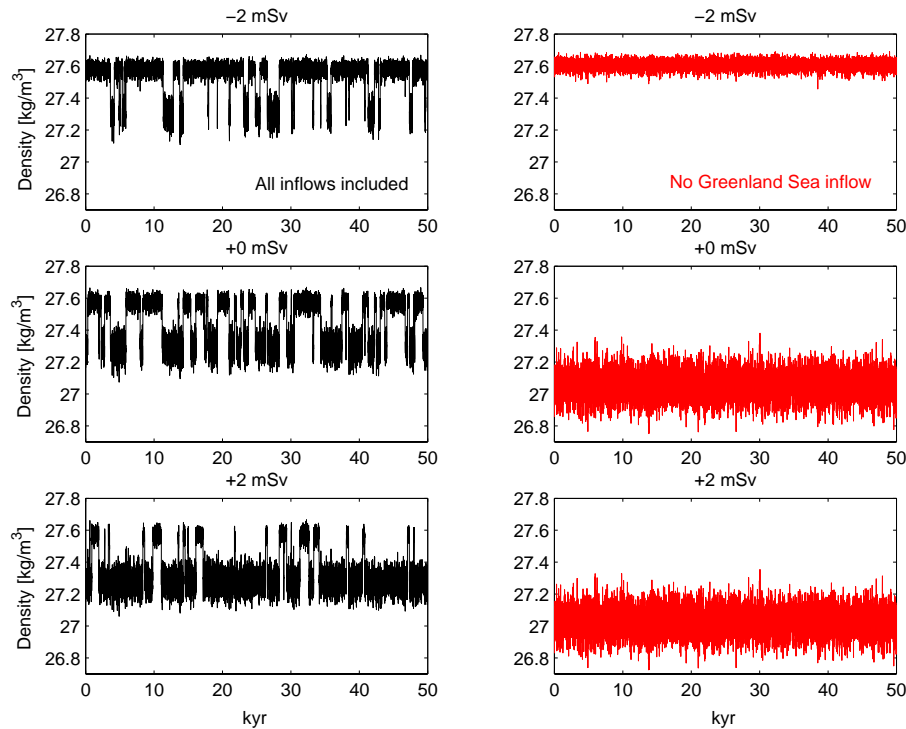


**Fig. 8.** Typical time series of Labrador Sea density anomalies in the stochastically forced ( $\sigma=0.2$  Sv) conceptual model with (black, left column) all inflows included and (red, right column) Greenland Sea inflow set to zero. From top to bottom, the additional constant freshwater influx  $P'$  increases from  $-2$  mSv to  $+2$  mSv.

[Title Page](#)
[Abstract](#)
[Introduction](#)
[Conclusions](#)
[References](#)
[Tables](#)
[Figures](#)
[◀](#)
[▶](#)
[◀](#)
[▶](#)
[Back](#)
[Close](#)
[Full Screen / Esc](#)
[Printer-friendly Version](#)
[Interactive Discussion](#)

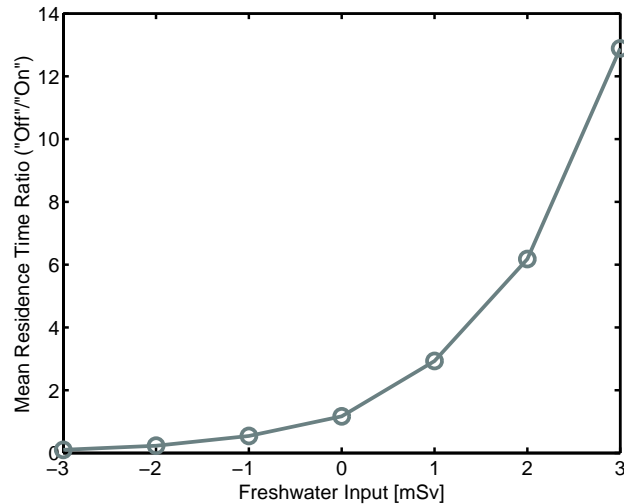


**Fig. 9.** Relation between the mean residence time ratio (i.e. the ratio between the mean residence times in the “off” mode and the “on” mode) and the constant freshwater input  $P'$  in the stochastically forced ( $\sigma=0.2$  Sv) conceptual model.

[Title Page](#)[Abstract](#)[Introduction](#)[Conclusions](#)[References](#)[Tables](#)[Figures](#)[◀](#)[▶](#)[◀](#)[▶](#)[Back](#)[Close](#)[Full Screen / Esc](#)[Printer-friendly Version](#)[Interactive Discussion](#)

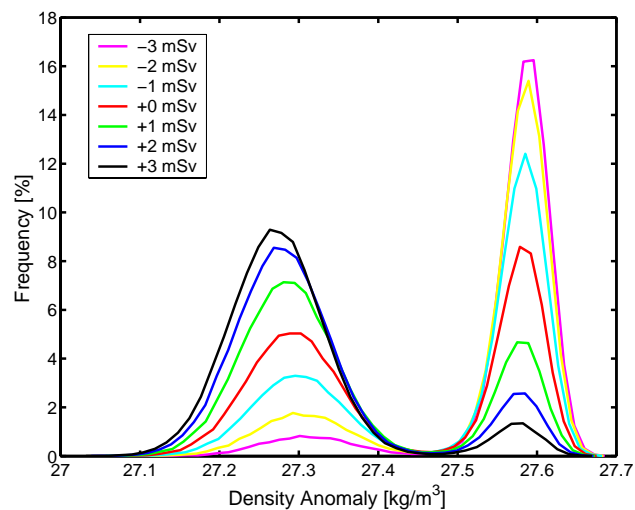


**Fig. 10.** Histograms (probability density functions) of Labrador Sea density-anomalies in the stochastically forced ( $\sigma=0.2$  Sv) conceptual model for different constant freshwater perturbations  $P'$  between  $-3$  mSv and  $+3$  mSv.

[Title Page](#)[Abstract](#)[Introduction](#)[Conclusions](#)[References](#)[Tables](#)[Figures](#)[◀](#)[▶](#)[◀](#)[▶](#)[Back](#)[Close](#)[Full Screen / Esc](#)[Printer-friendly Version](#)[Interactive Discussion](#)

## AMOC Oscillations

M. Schulz et al.

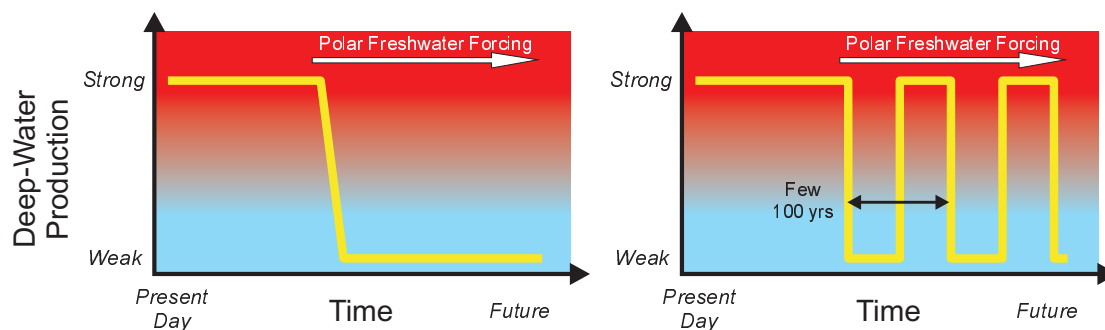


**Fig. 11.** A frequently invoked scenario for future climate change posits that enhanced freshwater input into polar regions results in a weakening of North Atlantic deep-water production (left). In contrast, our model results suggest an alternative route for future climate change involving oscillations in deep-water production at multicentennial timescales (right).

[Title Page](#)
[Abstract](#)
[Introduction](#)
[Conclusions](#)
[References](#)
[Tables](#)
[Figures](#)
[◀](#)
[▶](#)
[◀](#)
[▶](#)
[Back](#)
[Close](#)
[Full Screen / Esc](#)
[Printer-friendly Version](#)
[Interactive Discussion](#)